Application of a new 68Ga-labeled cNGR dimer peptide to microPET imaging of ovarian cancer

Yi Yang
the Affiliated Suzhou Science & Technology Town Hospital of Nanjing Medical University
Jun Zhang (dr.junzhang@hotmail.com)
Taizhou People's Hospital https://orcid.org/0000-0001-9761-2502
Huifeng Zou
the Affiliated Suzhou Science & Technology Town Hospital of Nanjing Medical University
Yang Shen
the Affiliated Suzhou Science & Technology Town Hospital of Nanjing Medical University
Yiwei Wu
the First Affiliated Hospital of Soochow University

Original research

Keywords: tumor angiogenesis, NGR peptide, CD13, microPET imaging, 68Ga labeling

Posted Date: March 20th, 2020

DOI: https://doi.org/10.21203/rs.3.rs-17734/v1

Abstract

Introduction: Peptides containing the asparagine-glycine-arginine (NGR) sequence have been found to specifically bind to cluster of differentiation 13 (CD13) (aminopeptidase N), a tumor neovascular biomarker that is overexpressed on the surface of angiogenic blood vessels and various tumor cells and plays an important role in angiogenesis and tumor progression. The aim of this study was to evaluate the efficacy of a gallium-68 (68 Ga)-labeled dimeric cyclic NGR (cNGR) peptide as a new molecular probe that binds to CD13 in vitro and in vivo .

Materials and Methods: A dimeric cNGR peptide conjugated with 1,4,7,10-tetraazacyclododecane-N,N',N",N"'-tetraacetic acid (DOTA) and DOTA-c(NGR) 2 was synthesized and labeled with 68 Ga. In vitro uptake and binding analysis was performed in two ovarian tumor cell lines, ES2 and SKOV3, each of which have different expression levels of CD13. An in vivo biodistribution study was performed in normal mice, and micro positron emission tomography (PET) imaging was performed in nude mice xenografts with ES2 and SKOV3 tumors.

Results : 68 Ga-DOTA-c(NGR) 2 with high radiochemical purity (>95%) was obtained and found to be stable at room temperature and when incubated with bovine serum at 37°C for 3 h. In vitro studies showed that uptake of 68 Ga-DOTA-c(NGR) 2 in ES2 cells increased over time, was higher than that in SKOV3 cells at all time points, and could be blocked by cold DOTA-c(NGR) 2 . Biodistribution studies demonstrated that 68 Ga-DOTA-c(NGR) 2 was mainly excreted from the kidney and rapidly cleared from blood. MicroPET imaging of ES2 tumor xenografts showed that focal uptake in tumors was distinctly observed from 1 to 1.5 h post-injection of 68 Ga-DOTA-c(NGR) 2 . Clear and high-contrast tumor visualization occurred at 1 h, which corresponded to the highest tumor/background ratio of 10.30±0.26. Moreover, accumulation of the probe in ES2 tumors apparently declined with pretreatment of unlabeled peptide, which further proved the specificity of 68 Ga-DOTA-c(NGR) 2 . In SKOV3 tumor models, the tumor was not obviously displayed under the same imaging protocols.

Conclusion : We conclude that 68 Ga-DOTA-c(NGR) 2 might be a potential molecular probe for evaluating the expression levels of CD13 in different tumors, thereby providing a basis for targeting angiogenesis in cancer therapy.

1. Introduction

Angiogenesis, the formation of new vessels from the preexisting vascular system, is the basic process of tumor progression. Studies have shown that tumor angiogenesis is a complex multistep process that is mediated and controlled by multiple adhesion molecules and cell receptors. Thus, targeting tumor angiogenesis with anti-angiogenic agents represents a promising therapeutic strategy for cancer control and treatment. Aminopeptidase N, also known as cluster of differentiation 13 (CD13), a zinc-dependent membrane-bound exopeptidase, is usually upregulated on the endothelium of tumor neovasculature and in various solid cancers including melanoma, prostate, ovarian, lung, and breast [1–4]. CD13 is a key

regulator implicated in angiogenesis and tumor progression, as well as a key binding receptor for peptides containing the asparagine-glycine-arginine (NGR sequence) [5–7]. In recent years, NGR peptide-based drug delivery and imaging studies have becoming an intriguing approach in cancer therapy and diagnosis. Molecular imaging of CD13 expression level is of great significance for guiding and monitoring the anti-angiogenesis therapy of NGR peptide-based drug delivery.

Ovarian cancer (OVCA), a serious threat to women's health, is characterized by high mortality and a high recurrence rate. It is the third most common gynecologic malignant tumor after endometrial carcinoma and cervical cancer in China, but its mortality rate is the highest of all gynecological malignancies [8]. Because CD13 is also expressed in OVCA and is involved in tumor progression, many studies have focused on treating OVCA by targeting CD13 [4, 9, 10]. However, due to the heterogeneity of the disease, CD13 is differentially expressed in OVCA tissues and cell lines such as ES2 and SKOV3 cells. ES2 cells are intensely positive for CD13, while SKOV3 cells express CD13 at a low levels [11].

In our previous study, gallium-68 (^{68} Ga)-labeled NGR linear monomer (^{68}Ga-1,4,7,10-tetraazacyclododecane-N,N',N'',N'''-tetraacetic acid [DOTA]-NGR) was applied in A549 lung cancer xenografts [12], and was found to be concentrated in the tumor. However, the retention time of the probe in the tumor was short, so translation to clinic would be difficult. We expect to improve the biodistribution and pharmacokinetics of the probe through further modification. Some reports have shown that cyclic peptides are more stable than linear ones because cyclic peptides are not easily broken down by enzymes [13]. In addition, the dimer has higher affinity to targets than the monomer because the dimer can bind more sites in target cells [14–15].

In this study, we designed and synthesized a novel radioactive molecular probe, a dimer of cyclic NGR (cNGR) peptide radiolabeled with ^{68}Ga, and applied it to micro positron emission tomography (PET) imaging of OVCA xenografts to evaluate its ability to identify tumors with CD13 expression at different levels.

2. Materials And Methods

2.1. General

All chemicals (reagent grade), unless specifically stated, were from commercial suppliers and no further purification was required. DOTA-c(NGR)$_2$ (Fig. 1) was commissioned by Sangon-Peptide Biotech Co., Ltd. (Ningbo, China) to synthesize using standard F-moc solid-phase chemistry. The yield was analyzed by high-performance liquid chromatography (HPLC) and mass spectrometry (MS) with a purity of more than 98%. $^{68}GaCl_3$ was produced from ^{68}Ge-^{68}Ga radionuclide generator (ITG GmbH, Oberding, Germany) by elution with 5 mL of 0.05 M HCl.

2.2. Labeling and characterization of ^{68}Ga-DOTA-c(NGR)$_2$

A concentration of 10 mg DOTA-c$(NGR)_2$ was dissolved in 2 mL deionized water to make a 5 mg/mL solution. Then 80 μL of 1 mol/L HEPES (pH 5.0, Sigma-Aldrich Corporation, St. Louis, MO, USA) was added to 200 μL $^{68}GaCl_3$ (37–74 MBq) eluent, and then incubated with 40 μL DOTA-c$(NGR)_2$ solution at 95 °C water bath for 10 min. Quality control was performed by radio-HPLC (Agilent Technologies, Santa Clara, CA, USA) with the VP-ODS C18 column (Shimadzu, Kyoto, Japan) and radioactivity detector (Zonkia Scientific Instruments Co., Ltd., Anhui Province, China). Mobile phase A was water with 0.1% trifluoroacetic acid (TFA) and mobile phase B was acetonitrile with 0.1% TFA. The flow rate was 1 mL/min and peaks were detected at 220 nm, with the mobile phase starting from 80% solvent A and 20% solvent B to 30% solvent B at 20 min. To evaluate in vitro stability, ~ 3.7 MBq of ^{68}Ga-DOTA-c$(NGR)_2$ were incubated in phosphate-buffered saline (PBS) at room temperature and in bovine serum at 37 °C, and radiochemical purity was measured at 30-min and 1-, 2-, and 3-h time points.

2.3. Cell culture and animal model

The human ovarian cancer ES2 and SKOV3 cells were obtained from Nanjing Keygen Biotech Co., Ltd. (Nanjing, China). ES2 cells were grown as monolayer cultures in McCoy's medium 5A containing 10% fetal bovine serum (FBS), and SKOV3 cells were cultured in RPMI 1640 medium containing 10% FBS. Both cell lines were incubated at 37 °C in a humidified atmosphere containing 5% CO_2. Cells in log phase were collected and prepared at a concentration of 5×10^7 /mL in PBS. A volume of 0.1 mL single-cell suspension was injected subcutaneously into the front flank of each female BALB/c-neu nude mouse (~ 4–6 weeks old, body weight of 18–25 g; Slac Laboratory Animal, Shanghai, China). Animal models were used for experiments when xenografts grew to 500–1000 mm^3. All animal studies were performed according to a protocol approved by the Institutional Animal Care and Use Committee of Soochow University.

2.4. Flow cytometry analysis

ES2 and SKOV3 cells were harvested by trypsinization and washed twice with PBS. The cells were adjusted to a concentration of 2×10^5 /mL with PBS. The cells were labeled with mouse-anti-human CD13 monoclonal antibody and incubated at 4 °C for 30 min. The superfluous antibodies were washed away by adding 1 mL cold PBS to each tube. The second antibody labeled with phycoerythrin was added and incubated at 4 °C for 30 min. The cells were washed twice and resuspended in 500 μL PBS. Then labeled cells were analyzed on a flow cytometer (FC-500; Beckman Coulter Inc., Sykesville, MD, USA) to quantify the expression level of CD13 on OVCA cells.

2.5. Immunohistochemical staining

Tumors were excised and fixed in 4% buffered formalin (pH 7.0). Sections of paraffin-embedded tumor tissues were baked in an oven at 65 °C for 2 h, dewaxed by being soaked with dimethylbenzene twice, and dehydrated using deionized water and alcohol washes of increasing concentrations (80%, 95%, and 100%). Antigens on the sections were retrieved with antigen repair solution (0.01 M citric acid buffer, pH 6.0) and endogenous peroxidase activity was eliminated with 3% freshly prepared H_2O_2. After blocking in

3% BSA (SW3015; Solarbio, Beijing, China) at 37 °C for 30 min, sections were incubated with adequate diluted rabbit anti-CD13 (1:150; Nanjing Keygen Biotech) in a wet box at 4 °C for 12 h, followed by the addition of polymeric horseradish peroxidase-labeled rabbit IgG as secondary antibody. After incubation for 30 min at 37 °C and three washes with PBS, sections were stained with a substrate-chromogen solution containing 0.025% 3, 3'-diaminobenzidine for 10 min and counterstained with hematoxylin for 3 min before microscope observation at low (200×) and high (400×) magnifications.

2.6. In vitro cell binding assay

To study the in vitro binding affinity and specificity of ^{68}Ga-DOTA-c(NGR)$_2$ to CD13, ES2 and SKOV3 cells were seeded into 6-well plates at 1 × 10^6 cells/well and cultured overnight. Then 37 KBq ^{68}Ga-DOTA-c(NGR)$_2$ was added and incubated at 37 °C for 5, 15, 30 min, 1, and 2 h after which the supernatant was suctioned, and cells were washed three times with PBS and harvested with 0.25% trypsin. Both the supernatant and cell suspensions were collected and counted using a gamma counter (CRC-55tR; Capintec, Florham Park, NJ, USA). Cell-based competitive binding assay was performed with ES2 cells. The cells were incubated with 37 KBq ^{68}Ga-DOTA-c(NGR)$_2$ in the presence of increasing concentrations of unlabeled DOTA-c(NGR)$_2$ (0.2–3.2 μg/mL). After 2 h of incubation at 37 °C, cells in all phases were collected and measured by the same previous method. The data were fitted with nonlinear regression using GraphPad Prism 7.0 (GraphPad Software, San Diego, CA, USA) to obtain the 50% inhibitory concentration (IC_{50}). Studies were performed in triplicate.

2.7. Biodistribution studies

Biodistribution studies were performed in 30 normal ICR (Institute of Cancer Research) mice (18–30 g; age, 4 weeks). At 10, 30, 60 min, and 2 h after injection of 3.7 MBq/0.1 mL ^{68}Ga-DOTA-c(NGR)$_2$ via the tail vein, mice (n = 6 per time point) were sacrificed by cervical dislocation, after which the blood, muscle and other organs of interest (brain, heart, liver, lungs, spleen, pancreas, kidneys, stomach, small intestine, and femur) were immediately harvested, weighed, and counted with a gamma counter. Data were normalized to the time of injection and expressed as percent injected dose per gram (% ID/g).

2.8. MicroPET imaging and blocking experiments

Two groups of female Balb/c nude mice (n = 6/group) bearing ES2 tumor models were used to conduct static microPET imaging with the Inveon microPET scanner (Siemens Medical Solutions, Erlangen, Germany). The first group was injected with 7.4 MBq ^{68}Ga-DOTA-c(NGR)$_2$ via tail vein under anesthesia with 1–2% isoflurane, and a series of static image data, 10 min for each time point, were collected at 30 min, 1, 1.5, and 2 h post-injection. For blocking studies, the second group of mice was injected with 136.67 nmol (100 μg in 100 μL distilled water) unlabeled peptide via tail vein immediately followed by administration of ^{68}Ga-DOTA-c(NGR)$_2$, and then images were acquired at 30 min, 1, 1.5, and 2 h post-injection, each for 10 min. The images obtained were processed using Siemens Inveon Research Workplace 4.0 (IRW 4.0) and reconstructed using three-dimensional ordered subset expectation maximization. Regions of interest (ROIs) were drawn over the tumor (T) and muscle of the contralateral

forelimb and the latter served as background (B). Percent injected dose per gram (%ID/g) of tumors and the T/B ratio were measured. The same studies were repeated in female Balb/c nude mice bearing SKOV3 tumor models without blocking experiments.

2.9. Statistical analysis

All quantitative data are presented as the mean ± standard deviation (SD). Statistical analysis was conducted by one-way analysis of variance and the Student's t-test. $P < 0.05$ was considered statistically significant.

3. Results

3.1. Radiochemistry and stability

Under the condition of bathing at 95 °C for 10 min, ^{68}Ga-DOTA-c(NGR)$_2$ was easily prepared with a high labeling rate of 98.01% ± 1.44%, and further purification was not needed. The retention time of labeling yields on radio-HPLC was 4.86 ± 0.27 min (Fig. 2). For the stability study, the radiochemical purity was > 96% in saline and > 95% in bovine serum after 3 h of incubation (Fig. 3).

3.2. Fluorescence-activated cell sorting and immunohistochemical staining

As shown in Fig. 2, fluorescence-activated cell sorting (FACS) revealed that expression rates of CD13 on ES2 cells and SKOV3 cells were 87.2% and 27.6% (Fig. 4), respectively. In accordance with the results of FACS, immunohistochemical staining showed that CD13 was significantly expressed on the membranes of the tumor and endothelial cells of the new vasculature in ES2 tumor tissue, at significantly higher levels than in SKOV3 tumor tissue (Fig. 5).

3.3. In vitro cell binding assay

Cell-binding studies were performed with ES2 cells and SKOV3 cells, and blocking studies were performed with ES2 cells. Significant binding differences were observed between ES2 cells and SKOV3 cells (Fig. 4). The results showed that the binding of ^{68}Ga-DOTA-c(NGR)$_2$ to ES2 cells increased over time with highest binding of 3.45% ± 0.51% achieved at 2 h of incubation, which was significantly higher than binding to SKOV3 cells at all time points with a highest binding of 1.79% ± 0.34% ($P < 0.05$) (Fig. 6). In blocking assays with excess cold peptide. ^{68}Ga-DOTA-c(NGR)$_2$ binding to ES2 cells significantly decreased at all time points with highest binding of 2.52% ± 0.15% ($P = 0.038$). Cell-based competitive binding assay in ES2 cells demonstrated that ^{68}Ga-DOTA-c(NGR)$_2$ binding was blocked by DOTA-c(NGR)$_2$ in a dose-dependent relationship, and the IC_{50} value was 160.1 nM (Fig. 7).

3.4. Biodistribution studies

The dynamic biodistribution results of ^{68}Ga-DOTA-c(NGR)$_2$ in healthy mice are shown in Fig. 5. Radiouptake in the kidney peaked at 5 min (16.7 ± 5.80% ID/g) and then rapidly decreased by more than 50% at 30 min and 85% at 120 min post-injection, followed by the liver and lung. Quick clearance of ^{68}Ga-DOTA-c(NGR)$_2$ from blood was observed, and the blood uptake was 7.44 ± 1.64% ID/g at 5 min and 0.31 ± 0.05% ID/g at 60 min post-injection. Activity in brain, heart, stomach, intestines, spleen, pancreas, and bone was markedly lower (Fig. 8).

3.5. MicroPET imaging and blocking experiments

After injection with ^{68}Ga-DOTA-c(NGR)$_2$, a series of microPET images from ES2 tumor-bearing mice were collected at 30 min, 1, and 1.5 h and were represented by coronal and transverse views (Fig. 6). High focal accumulation in tumor was visualized at 1 and 1.5 h and was then reduced at 2 h. Marked accumulation of radioactivity in the bladder was observed at all time points. With the exception of 30 min, distribution of radioactivity in liver was barely observed in subsequent images. Quantitative analysis by ROI technology revealed that the uptake of ^{68}Ga-DOTA-c(NGR)$_2$ in ES2 tumors was 0.62 ± 0.09% ID/g at 1 h and 0.53 ± 0.08% ID/g at 1.5 h, whereas in SKOV3 tumors it was 0.32 ± 0.03% ID/g and 0.24 ± 0.05% ID/g, respectively. The T/B ratio in ES2 tumors was 10.30 ± 0.26 at 1 h and 8.04 ± 1.75 at 1.5 h, but in SKOV3 tumors was 3.99 ± 0.18 and 4.24 ± 0.73, respectively. In ES2 tumors blocked by unlabeled peptide, it was only 0.16 ± 0.03% ID/g at 1 h and 0.14 ± 0.02% ID/g at 1.5 h. (Fig. 9)

Discussion

Although to date, no antiangiogenic agents can eradicate tumors alone, effective inhibition of tumor angiogenesis might arrest tumor progression and has been shown to synergize with other cancer treatments [16–17]. As one targeted tumor therapy, only a few patients can actually benefit from antiangiogenic therapy due to the biological heterogeneity of tumors [18–19]. Molecular imaging using radioisotopes labeled with targeted drugs or its analogs makes it possible to select patients, predict efficacy, and dynamically assess response to therapy [20]. Detection of specific molecular targets is an important application of molecular imaging in the management of malignancies.

In nuclear medicine, PET has become a very important imaging technique for the diagnosis and treatment efficacy evaluation of cancer. Currently, ^{18}F-FDG is still the most widely used radiotracer for PET imaging. The acquisition of ^{18}F-FDG depends on the availability of a nearby cyclotron. Due to the high price and operating cost of the cyclotron, only a small number of medical institutions has both a PET and cyclotron. Moreover, ^{18}F-FDG traces tumor cell glucose metabolism and is used for the diagnosis and evaluation of therapeutic effects. It is a non-specific tumor imaging agent, which limits its application to guide targeted therapy, especially selecting the right patients.

^{68}Ga, a generator-based positron radioisotope, is relatively easy to obtain by ^{68}Ge/^{68}Ga radionuclide generators and shows equally high-quality images on PET. $^{68}Ga^{3+}$ can form stable complexes with many ligands containing oxygen and nitrogen as donor atoms by aid of chelators, which makes it an appealing alternative to ^{18}F [21].

Radioisotope-labeled RGD peptides have been widely studied as molecular probes for tumor angiogenesis imaging [22–25]. However, RGD targets integrin αvβ3, which works well for tumors with positive expression of integrin αvβ3, but cannot be used for tumors that do not express or have low expression of αvβ3. CD13 is another important target of tumor and angiogenesis, and NGR can be specifically combined with CD13 to form a new probe, which can be an important complement to the RGD probe. To improve the targeting and biological metabolic characteristics of the NGR probe, we refer to the successful experience of RGD modification. The cyclic dimer peptide has a more stable structure and higher affinity than the monomer, and PEG modification can increase the hydrophobicity of peptides and thus improve the pharmacokinetics of the probe [13, 26]. In this study, we designed a cyclic NGR dimer linked by PEG-4 and labeled it with ^{68}Ga to form a new radiolabeled probe targeting CD13.

^{68}Ga-DOTA-c(NGR)$_2$ with high radiochemical purity was obtained after relatively simple labeling steps without further purification, and the yield maintained stability in bovine serum beyond 3 h. To verify the specificity and cellular binding kinetics of the probe, two ovarian cancer cell lines, ES2 cells and SKOV3 cells, expressing CD13 at significantly different levels were utilized to mimic heterogeneity from the same tumor. An in vitro binding assay demonstrated that the binding of ^{68}Ga-DOTA-c(NGR)$_2$ to ES2 cells was significantly higher than that in SKOV3 cells and could be inhibited with unlabeled DOTA-c(NGR)$_2$ in a dose-dependent relationship, which revealed the specificity of ^{68}Ga-DOTA-c(NGR)$_2$ to CD13-positive tumor cells in vitro. The results suggested that ^{68}Ga-DOTA-c(NGR)$_2$ could be used to identify tumors with high expression of CD13 by PET imaging in vivo.

Biodistribution studies demonstrated that a large proportion of ^{68}Ga-DOTA-c(NGR)$_2$ was metabolized through the urinary system and rapidly cleared from blood, whereas its early uptake in other organs such as liver, lungs, and spleen was probably correlative to the blood supply of these organs. The distribution characteristics were also confirmed by subsequent imaging studies of tumor xenografts. Series of microPET images of ES2 tumor model showed that focal uptake in the tumor was distinctly observed from 1 h post-injection of ^{68}Ga-DOTA-c(NGR)$_2$. Meanwhile, ^{68}Ga-DOTA-c(NGR)$_2$ started to accumulate in the bladder from 30 min. Clear and high-contrast tumor visualization occurred at 1 h, which corresponded to the highest T/B ratio of 10.30 ± 0.26. Moreover, accumulation of ES2 tumor apparently declined by pretreatment of unlabeled peptide, which further proved the specificity of ^{68}Ga-DOTA-c(NGR)$_2$. In SKOV3 tumor models, the tumor was not clearly seen under the same imaging conditions.

In our previous study, ^{68}Ga labeling linear NGR conjugated with DOTA, ^{68}Ga-DOTA-NGR, was synthesized, which showed high selectivity and affinity for CD13 and in significant uptake in CD13-positive lung tumors [12]. Compared with this study, a cNGR dimer was used and its higher affinity to CD13 and higher uptake in tumors were observed, consistent with our prediction. However, we noted that the uptake decreased in the tumor at 2 h post-injection. Further optimization of the structure of the probe may improve its pharmacokinetic characteristics and increase affinity to CD13-positive tumors.

It is worth noting that our work is only a preliminary study on the physicochemical and biological characteristics of a newly designed cyclic dimer probe based on the NGR sequence. It was not compared with other probes of NGR derivatives in previous studies under the same experimental conditions.

Conclusion

^{68}Ga-DOTA-c(NGR)$_2$ are easily synthesized with high radiochemical purity and stability. Due to its high selectivity and affinity for CD13, ^{68}Ga-DOTA-c(NGR)$_2$ might be a potential molecular probe for evaluating CD13 expression levels in different tumors, thereby providing a basis for targeted therapy.

Abbreviations

^{68}Ga gallium-68

NGR asparagine-glycine-arginine

cNGR cyclic NGR

cNGR2 cyclic NGR dimer

DOTA 1,4,7,10-tetraazacyclododecane-N,N’,N”,N”’-tetraacetic acid

PET Positron emission tomography

CD13 cluster of differentiation 13

OVCA Ovarian cancer

FBS fetal bovine serum

% ID/g percent injected dose per gram

ROI Region of interest

FACS fluorescence-activated cell sorting

Declarations

Ethics approval and consent to participate

All animal studies were performed according to a protocol approved by the Institutional Animal Care and Use Committee of Soochow University.

Consent for publication

Not applicable.

Availability of data and materials

The datasets supporting the results of this article are included within the manuscript and its additional files.

Competing interests

The authors declare that they have no competing interests.

Funding

This work was supported by grants from the Natural Science Foundation of Jiangsu Province (No. BK20151352 to Jun Zhang), Young Medical Key Talents Project of Jiangsu province (No. QNRC2016515 to Jun Zhang), "Six Ones Project" high-level top medical talent project of Jiangsu province (No. LGY2017032 to Jun Zhang), the Suzhou Science and Technology Development Plan (No. SYSD2017066 to Yi Yang), and the Suzhou New District Science and Technology Plan (No.2016Z0004 to Yi Yang).

Authors' contributions

YY: contributor in cell culture and animal experiment, data analysis, and writing of the manuscript. JZ: contributor in study design, radiolabeling of peptides, data analysis and interpretation, and writing and critical revision of the manuscript. HZ: contributor in micro PET acquisition and data analysis. YS: contributor in flow cytometry analysis, H&E staining, histopathological data acquisition. YW: contributor in study design and revision of the manuscript. All authors read and approved the final manuscript.

Acknowledgements

We thank LetPub (www.letpub.com) for its linguistic assistance during the preparation of this manuscript.

Disclosure Statement

No competing financial interests exist.

References

1. Tokuhara T, Hattori N, Ishida H, Hirai T, Higashiyama M, Kodama K, et al (2006) Clinical significance of aminopeptidase N in non-small cell lung cancer. Clin Cancer Res 12:3971-3978.
2. Hashida H, Takabayashi A, Kanai M, Adachi M, Kondo K, Kohno N, Yamaoka Y, et al (2002) Aminopeptidase N is involved in cell motility and angiogenesis: its clinical significance in human colon cancer. Gastroenterology 122: 376-386.

3. Ishii K, Usui S, Sugimura Y, Yoshida S, Hioki T, Tatematsu M, et al (2001) Aminopeptidase N regulated by zinc in human prostate participates in tumor cell invasion. Int J Cancer 92(1):49-54.
4. Terauchi M, Kajiyama H, Shibata K, Ino K, Nawa A, Mizutani S, et al (2007) Inhibition of APN/CD13 leads to suppressed progressive potential in ovarian carcinoma cells. BMC Cancer 7:140.
5. Sjöström H, Norén O, Olsen J (2000) Structure and function of aminopeptidase N (2008) Adv Exp Med Biol 477:25-34.
6. Mina-Osorio P. The moonlighting enzyme CD13: old and new functions to target.Trends Mol Med;14:361-71.
7. Hashida H, Takabayashi A, Kanai M, Adachi M, Kondo K, Kohno N, et al (2002) Aminopeptidase N is involved in cell motility and angiogenesis: its clinical significance in human colon cancer. Gastroenterology 122:376-86.
8. Cortez AJ, Tudrej P, Kujawa KA, Lisowska KM, et al (2018) Advances in ovarian cancer therapy. Cancer Chemother Pharmacol 81:17-38.
9. Gao JJ, Gao ZH, Zhao CR, Yuan Y, Cui SX, Zhang XF, et al (2011) LYP, a novel bestatin derivative, inhibits cell growth and suppresses APN/CD13 activity in human ovarian carcinoma cells more potently than bestatin. Invest New Drugs 29:574-582.
10. Cui SX, Qu XJ, Gao ZH, Zhang YS, Zhang XF, Zhao CR, et al (2010) Targeting aminopeptidase N (APN/CD13) with cyclic-imide peptidomimetics derivative CIP-13F inhibits the growth of human ovarian carcinoma cells. Cancer Lett 292:153-162.
11. Pasqualini R, Koivunen E, Kain R, Lahdenranta J, Sakamoto M, Stryhn A, et al (2000) Aminopeptidase N is a receptor for tumor-homing peptides and a target for inhibiting angiogenesis. Cancer Res 60:722-727.
12. Zhang J, Lu X, Wan N, Hua Z, Wang Z, Huang H, et al. ^{68}Ga-DOTA-NGR as a novel molecular probe for APN-positive tumor imaging using MicroPET. Nucl Med Biol 2014;41:268-75.
13. Colombo G, Curnis F, De Mori GM, Gasparri A, Longoni C, Sacchi A, et al (2002) Structure-activity relationships of linear and cyclic peptides containing the NGR tumor-homing motif. J Biol Chem 277: 47891-47897.
14. Chen K1, Ma W, Li G, Wang J, et al (2013) Synthesis and evaluation of 64Cu-labeled monomeric and dimeric NGR peptides for microPET imaging of CD13 receptor expression. Mol Pharm10:417-27.
15. Ma W, Kang F, Wang Z, et al (2013) 99mTc-labeled monomeric and dimeric NGR peptides for SPECT imaging of CD13 receptor in tumor-bearing mice. Amino Acids 44:1337-1345.
16. Jain RK, Duda DG, Willett CG, Sahani DV, Zhu AX, Loeffler JS, et al (2009) Biomarkers of response and resistance to antiangiogenic therapy. Nat Rev Clin Oncol 6:327-338.
17. Carmeliet P, Jain RK (2011) Molecular mechanisms and clinical applications of angiogenesis. Nature 473:298-307.
18. Cheng X, Chen H (2014) Tumor heterogeneity and resistance to EGFR-targeted therapy in advanced nonsmall cell lung cancer: challenges and perspectives. Onco Targets Ther 7:1689-1704.

19. Li D, Finley SD (2018) The impact of tumor receptor heterogeneity on the response to anti-angiogenic cancer treatment. Integr Biol (Camb) 10:253-269.
20. Choudhury P, Gupta M (2017) Personalized and precision medicine in cancer: a theragnostic approach. Curr Radiopharm 10:166-170.
21. Smith DL, Breeman WA, Sims-Mourtada J (2013) The untapped potential of Gallium 68-PET: The next wave of (68)Ga-agents. Appl Radiat Isot 76:14-23.
22. Haubner R, Wester HJ, Weber WA, Mang C, Ziegler SI, Goodman SL, et al (2001) Noninvasive imaging of alpha(v)beta3 integrin expression using 18F-labeled RGD-containing glycopeptide and positron emission tomography. Cancer Res 61:1781-1785.
23. Beer A J, Haubner R, Sarbia M, et al (2006) Positron emission tomography using [18F]Galacto-RGD identifies the level of integrin αvβ3 expression in man. Clin Cancer Res 12: 3942-3949.
24. McParland BJ, Miller MP, Spinks TJ, Kenny LM, Osman S, Khela MK, et al (2008) The biodistribution and radiation dosimetry of the Arg-Gly-Asp peptide 18F-AH111585 in healthy volunteers. J Nucl Med 49: 1664-1667.
25. Zhai C, Franssen GM, Petrik M, Laverman P, Summer D, Rangger C, et al (2016) Comparison of Ga-68-Labeled Fusarinine C-Based Multivalent RGD Conjugates and [(68)Ga]NODAGA-RGD-In Vivo Imaging Studies in Human Xenograft Tumors. Mol Imaging Biol 18:758-767.
26. Negussie AH, Miller JL, Reddy G, Drake SK, Wood BJ, Dreher MR, et al (2010) Synthesis and in vitro evaluation of cyclic NGR peptide targeted thermally sensitive liposome. J Control Release 143:265-273.

Figures

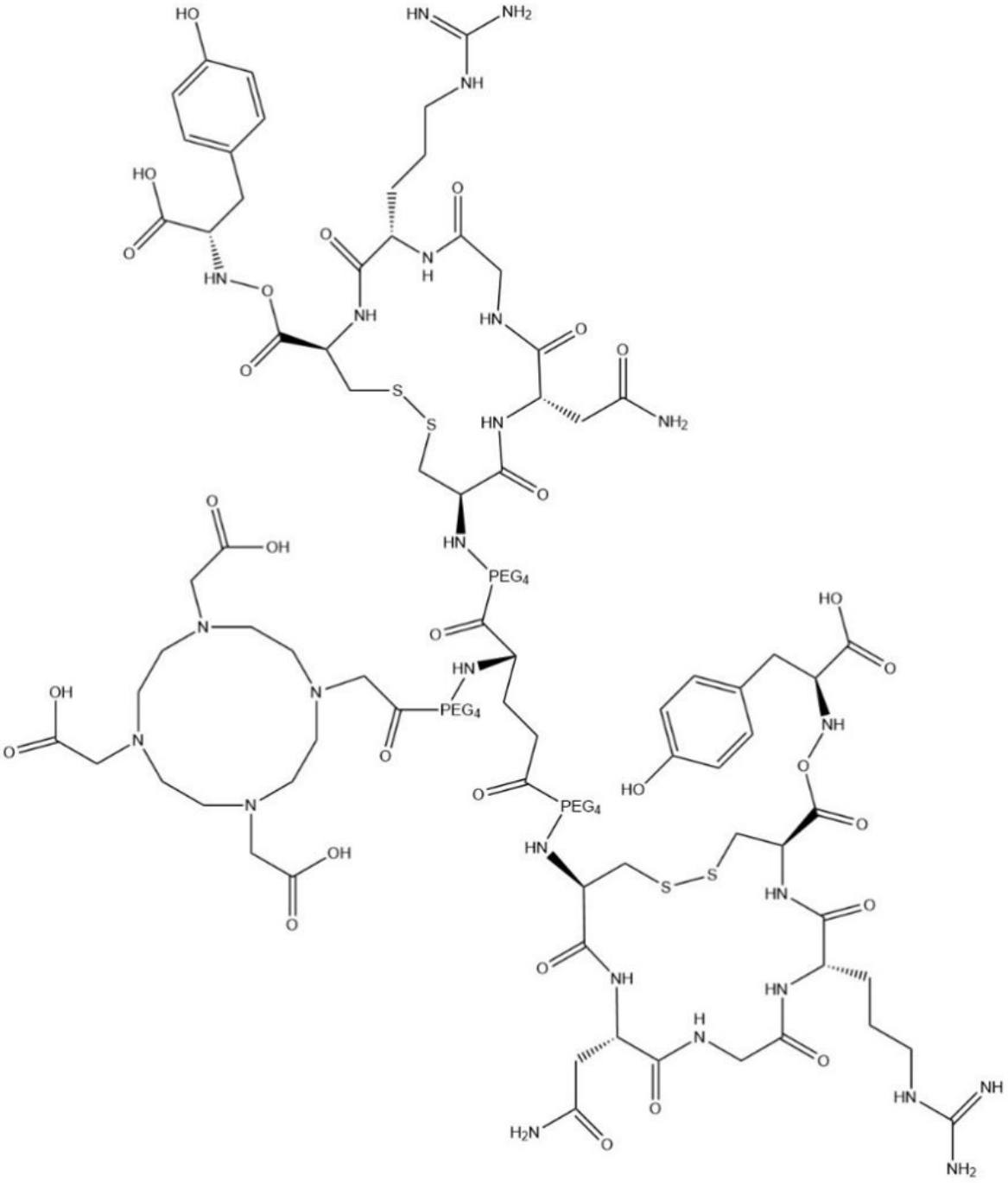

Figure 1

Structural formula of DOTA-c(NGR)2; chemical formula: C99H159N25O41S4; molecular weight: 2483.74.

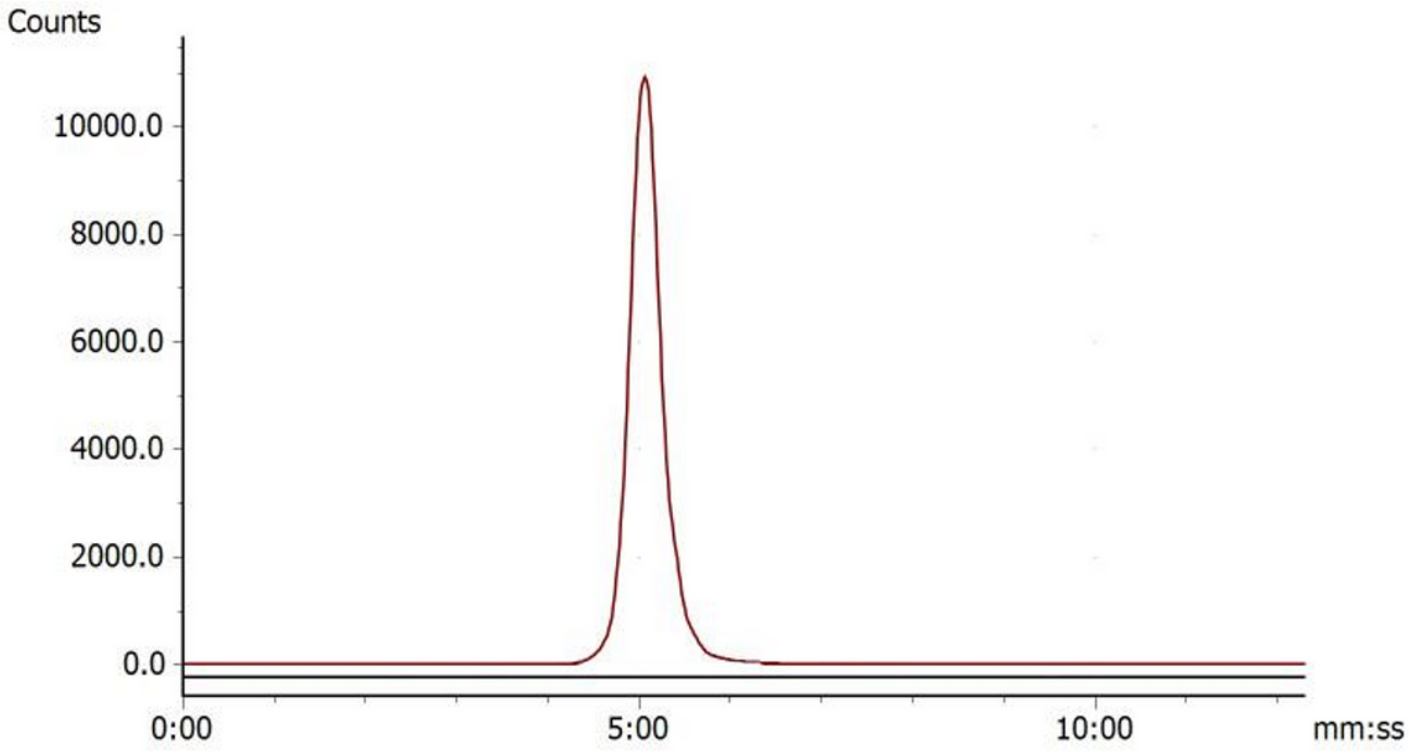

Figure 2

Radio-HPLC of 68Ga-DOTA-c(NGR)2 (retention time is 5.23 min).

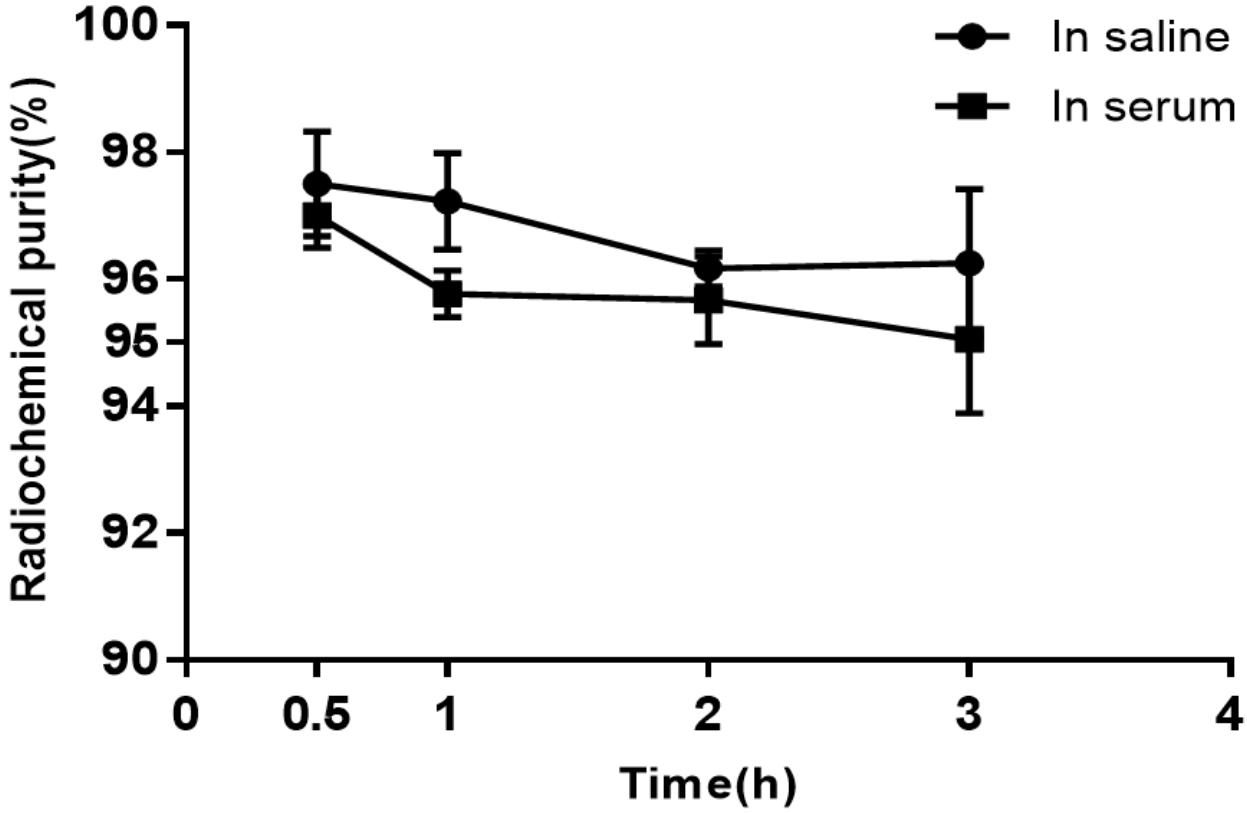

Figure 3

In vitro stability of 68Ga-DOTA-c(NGR)2 in saline at room temperature and in bovine serum at 37 °C for 30 min, 1 h, 2 h and 3 h.

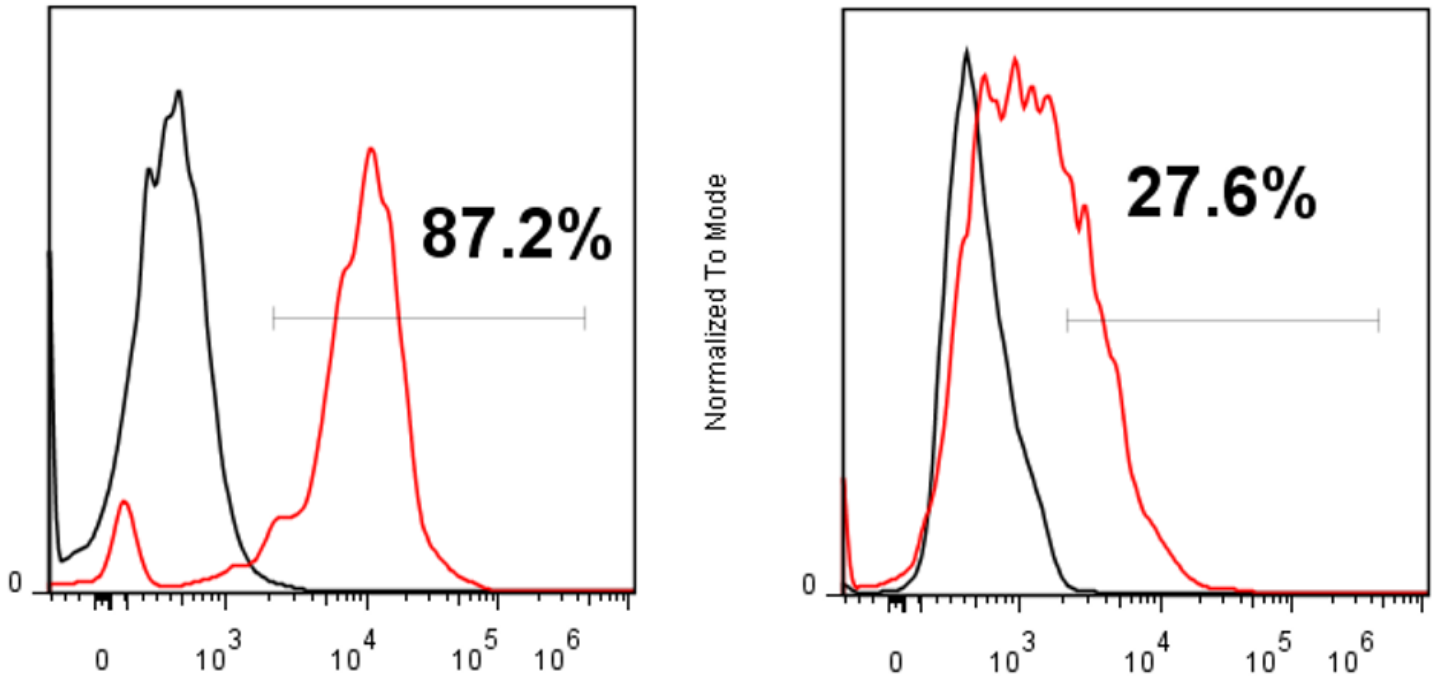

Figure 4

FACS analysis of CD13 expression on ES2 (A) and SKOV3(B) cells.

Figure 5

Immunohistochemical staining. (A) and (B) CD13 expression in SKOV3 tumor tissue sections; (C) and (D) CD13 expression in ES2 tumor tissues. (A and C Magnification × 200, B and D Magnification ×400).

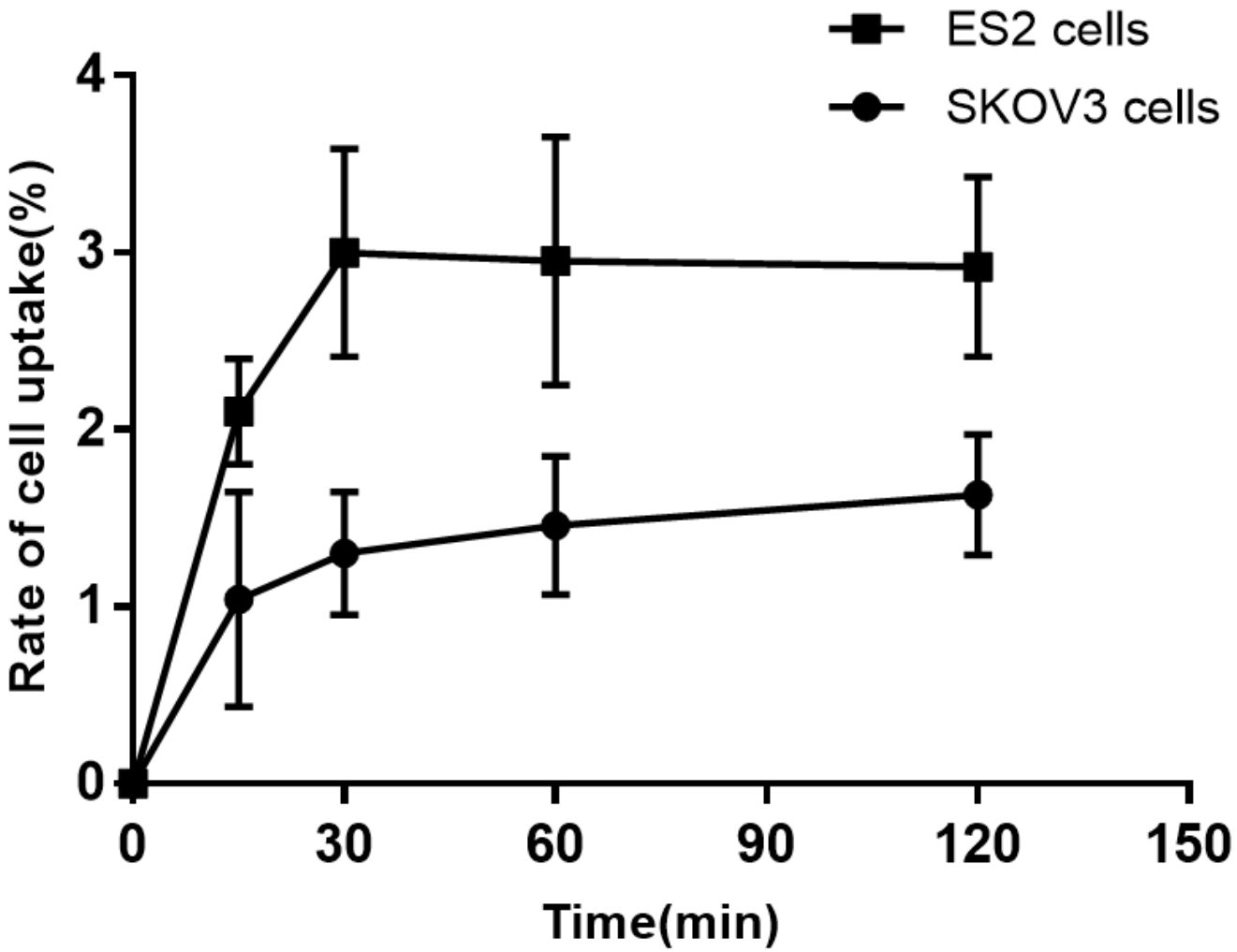

Figure 6

Uptake of 68Ga-DOTA-c(NGR)2 in ES2 and SKOV3 cells.

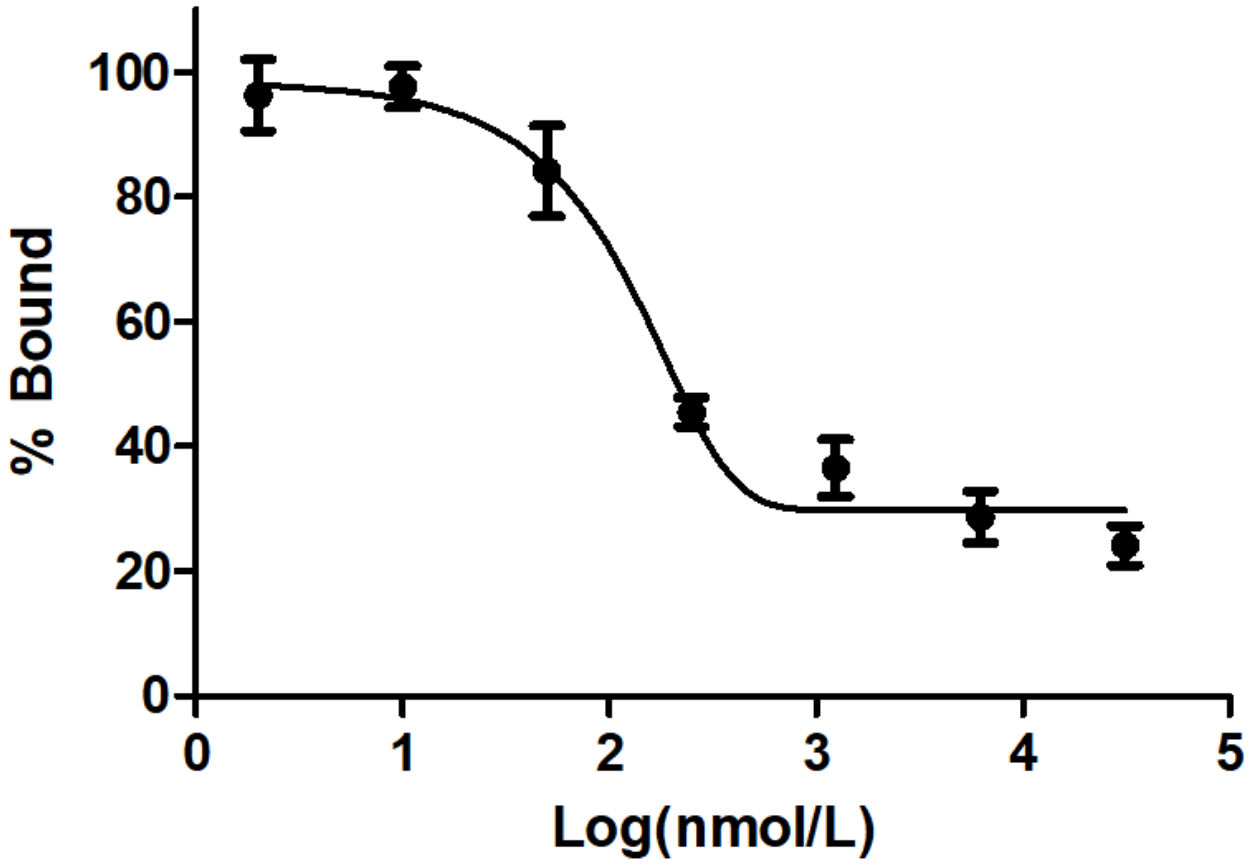

Figure 7

Competitive binding assay. The uptake in ES2 cells could be inhibited competitively by unlabeled DOTA-c(NGR)2 in dose-dependent manner, and the IC50 value was 160.1 nM.

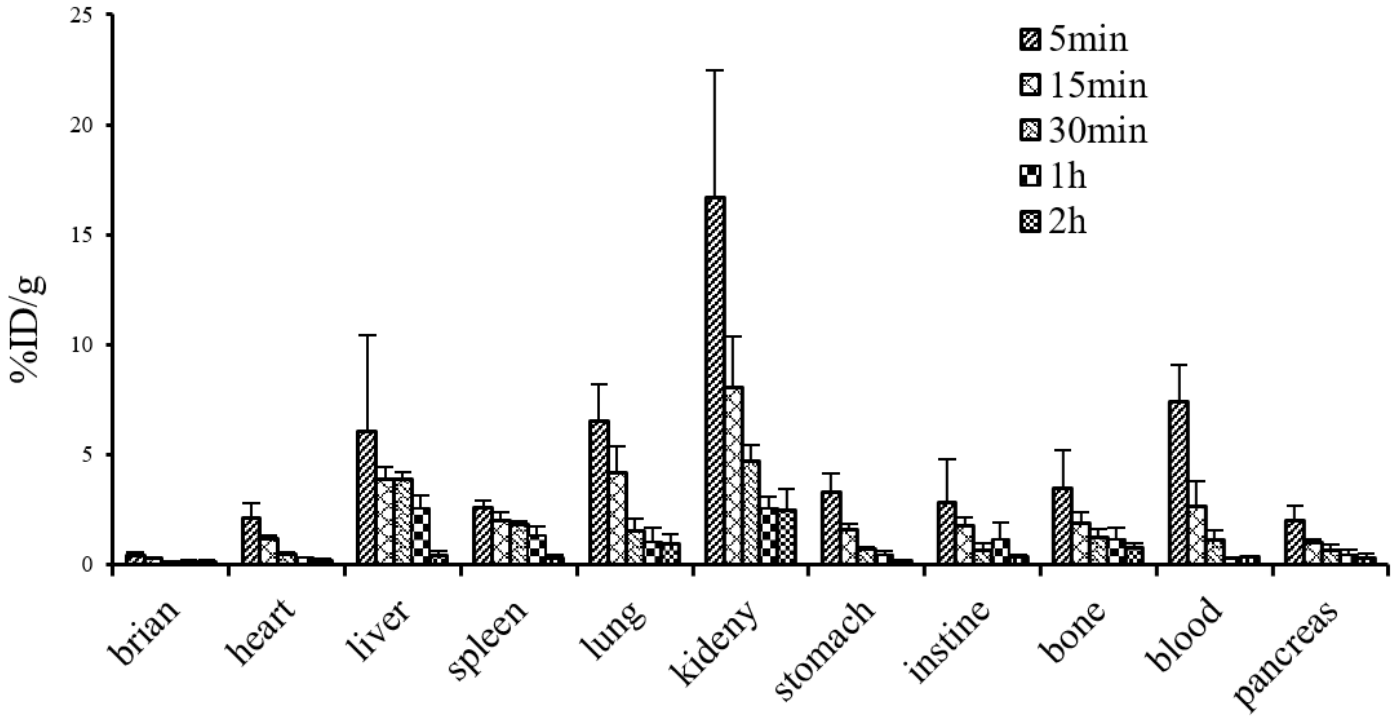

Figure 8

Biodistribution of 68Ga-DOTA-c(NGR)2 in normal mice.

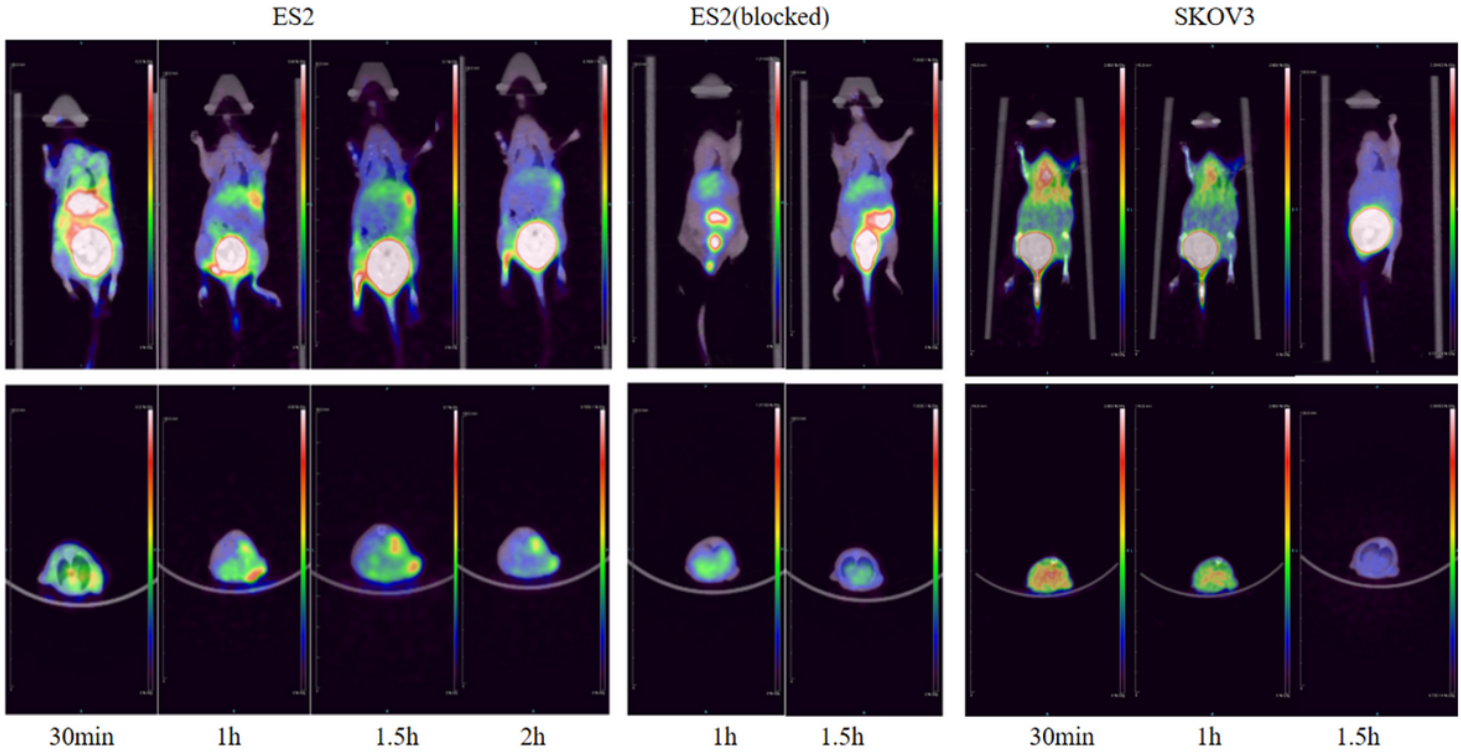

Figure 9

Representative microPET images of 68Ga-DOTA-c(NGR)2 in xenograft models.